Presented at the 32nd European PV Solar Energy Conference and Exhibition, 20-24 June 2016, Munich, Germany

IMPACT OF HIGH-TEMPERATURE PROCESSES ON CARRIER LIFETIME OF N-TYPE CZ SILICON

S. Werner[1], A. Wolf[1], S. Mack[1], E. Lohmüller[1], R.C.G. Naber[2]
[1]Fraunhofer Institute for Solar Energy Systems ISE, Heidenhofstraße 2, 79110 Freiburg, Germany
[2]Tempress Systems, Radeweg 31, 8171 MD Vaassen, The Netherlands
Phone: +49 761 4588 5049, e-mail: sabrina.werner@ise.fraunhofer.de

ABSTRACT: We investigate the impact of high-temperature processes on phosphorus-doped n-type Czochralski-grown silicon (Cz-Si) wafers. Wafers from five ingots are subjected to high-temperature process sequences with different temperatures, times, and gas atmospheres. The process sequences are specifically chosen to represent different routes for the fabrication of high-efficiency n-type Cz-Si solar cells. As $POCl_3$ diffusion is known for its effective gettering of metal impurities, it is preferably used as the last high-temperature step. However, our results show that other process sequences, e.g. with BBr_3 diffusion as last high-temperature step, enable high charge carrier lifetimes in the range of a few milliseconds as well. For some materials and process sequences, ring-shaped defect structures are observed while for others increased charge carrier lifetimes by a factor up to 2.6 are found compared to their initial values prior to high temperature processing.
Keywords: n-type, silicon, high-temperature processes, lifetime, precipitates, oxygen, $POCl_3$ diffusion, BBr_3 diffusion, nitrogen

1 INTRODUCTION

Phosphorus-doped n-type Czochralski-grown silicon (Cz-Si) wafers are often used in the fabrication of high-efficiency silicon solar cells due to the absence of light-induced degradation [1]. For processing n-type Cz-Si solar cells, typically high-temperature process steps form both the boron-doped emitter and the highly phosphorus-doped surfaces. These doped layers can be realized by, e.g., high-temperature tube furnace diffusion processes using BBr_3 and $POCl_3$ as liquid dopant precursors. Another option is the use of high-temperature tube furnace processes in O_2 or N_2 gas atmosphere, either to anneal crystal damage after ion-implantation or to drive in dopants from previously deposited or printed sources. However, these high-temperature processes may lead to a decrease in charge carrier lifetime in some n-type Cz-Si materials due to the formation of oxygen precipitates [2] or other defects. To overcome this issue, one may select either n-type Cz-Si material that does not degrade during high-temperature processing or process sequences that do not lead to a degradation of the bulk lifetime of n-type Cz-Si wafers.

This work presents a comprehensive study of the key components: n-type Cz-Si wafer materials and processing sequences. Therefore, we investigate n-type Cz-Si wafer sets from different ingots and suppliers with respect to their lifetimes before and after different high-temperature tube furnace process sequences.

2 APPROACH

2.1 High-temperature processes

For the fabrication of high-efficiency n-type silicon solar cells, different combinations of high-temperature processes are imaginable to form the phosphorus- and boron-doped regions. $POCl_3$ diffusion and ion-implantation of boron with subsequent high-temperature annealing or, on the other hand, BBr_3 diffusion and subsequent $POCl_3$ diffusion are two exemplary options.

For the material evaluation of n-type Cz-Si wafers, various combinations and sequences of BBr_3, $POCl_3$, O_2, and N_2 tube furnace processes at different peak temperatures T_{Peak} and peak times t_{Peak} are used; see Table I. Both the $POCl_3$ diffusion process and the BBr_3 diffusion process feature an *in-situ* oxidation [3–5] and are frequently applied in the PV-TEC laboratory at Fraunhofer ISE. The processes "O_2 low" and "N_2 low" have a similar thermal budget as the $POCl_3$ diffusion process, but for the process atmosphere we look at two extreme cases with pure O_2 or pure N_2 gas atmosphere. The processes "O_2 high" and "N_2 high" feature a higher thermal budget as the diffusion processes. Such processes might be applied to drive in the dopants from a previously deposited layer or to anneal/redistribute implanted dopants.

2.2 Sample preparation

Various n-type Cz-Si wafers with an edge length of 156 mm and different base resistivities ρ_{Base} are investigated with respect to their lifetimes before and after different high-temperature tube furnace process sequences; see Fig. 1. Therefore, two experiments are carried out. The first experiment focuses on the investigation of a wide range of different materials in high-temperature process sequences while the second experiment focuses on a broader investigation of high-temperature process sequences. Thus, in the first experiment wafers from five different ingots from four different suppliers (Mat1 – Mat5) are subjected to five high-temperature process sequences. In the second experiment, which includes eight additional high-temperature process sequences, only two materials (Mat1 and Mat2) are used. More details about the applied process sequences will follow with the discussion of the results. Each group contains four wafers per material.

First, ρ_{Base} of the wafers are measured by means of inductive coupling using an inline tool [6]. After random

Table I: Peak temperature T_{Peak}, peak time t_{Peak}, and the gas atmosphere of the used high-temperature processes.

Process name	T_{Peak} (°C)	t_{Peak} (min)	Gas atmosphere
$POCl_3$	860	12	$POCl_3$, O_2, N_2
BBr_3	955	20	BBr_3, O_2, N_2
O_2 low	860	12	pure O_2
O_2 high	1000	60	pure O_2
N_2 low	860	12	pure N_2
N_2 high	1000	60	pure N_2

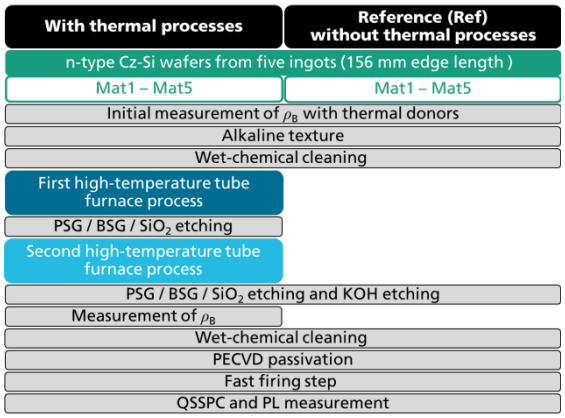

Fig. 1. Schematic process sequence used for the material evaluation of n-type Cz-Si wafers from five different ingots and four different suppliers (Mat1 – Mat5) in different high-temperature tube furnace process sequences (PSG: phosphosilicate glass, BSG: borosilicate glass, ρ_{Base}: base resistivity, PECVD: plasma-enhanced chemical vapor deposition, QSSPC: quasi-steady-state photoconductance, PL: photoluminescence). In a second experiment, which addresses additional high-temperature processes, only two materials (Mat1 and Mat2) are used.

pyramid formation in alkaline solution and wet-chemical cleaning, the wafers are subjected to one or two selected high-temperature processes such as BBr_3, $POCl_3$, O_2, or N_2 tube furnace processes at different T_{Peak} and t_{Peak} (see Table I). In between those two processes, the possibly formed phosphosilicate glasses (PSG), borosilicate glasses (BSG) or SiO_2 layers (depending on the used processes) are removed in HF solution. The two subsequently carried out high-temperature processes are referred to as "process1 + process2" (e.g. "BBr_3 + O_2 low"). The double-sided highly-doped regions after the initial $POCl_3$/BBr_3 diffusion are neither removed nor coated by diffusion barrier layers for the second high-temperature process. One reference group per material is not subjected to any high-temperature process.

After the high-temperature sequences, all surface oxide layers are removed in HF solution and the diffused and textured surfaces are subsequently etched back and smoothened in KOH solution (silicon removal of about 10 µm from each side resulting in a final wafer thickness $W \approx 150$ µm, also for the reference group). The used high-temperature processes dissolve any thermal donors which might have existed before. To determine information about the content of thermal donors per material, another measurement of ρ_{Base} is performed at this stage of the experiment.

Following wet-chemical cleaning, the alkaline saw-damage etched surfaces are passivated with a layer stack consisting of silicon-rich oxynitride (SiRiON) [7] and silicon nitride (SiN_x) deposited by PECVD. After activating the passivation layers in a fast firing furnace at a set peak temperature of 700°C, the effective charge carrier lifetime τ_{eff} is measured by QSSPC at five positions over each wafer and spatially resolved PL images are recorded. As all wafers are identically wet-chemically etched and passivated, we assume the surface recombination velocity to be very similar for all wafers. Therefore, we conclude that all correlations found for the measured effective lifetimes can be related to the silicon bulk.

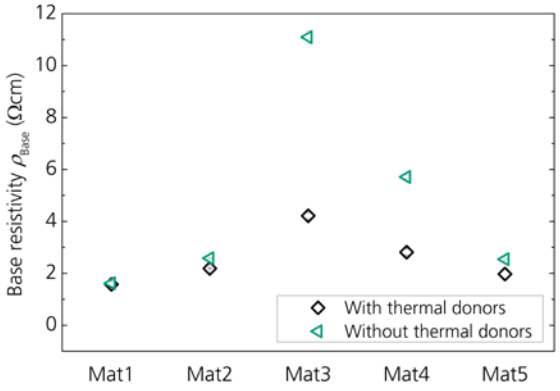

Fig. 2. Base resistivity ρ_{Base} of the wafers from five different n-type Cz-Si ingots investigated in this work with and without thermal donors, measured by means of inductive coupling [6].

3 RESULTS

3.1 Base resistivity with and without thermal donors

The base resistivities ρ_{Base} of the five n-type Cz-Si materials investigated in this work are shown in Fig. 2 with and without thermal donors. Thermal donors can be correlated to the oxygen content of the Cz-Si [8]. For Mat1, ρ_{Base} is determined to be $\rho_{Base} \approx 1.6$ Ωcm with and without thermal donors. Thus, the content of thermal donors within this material is marginal. In contrast, ρ_{Base} for Mat3 increases from $\rho_{Base} \approx 4.2$ Ωcm with thermal donors to $\rho_{Base} \approx 11.1$ Ωcm without thermal donors, which comes along with a high content of thermal donors. The different materials have been chosen such that the investigation includes materials with different amounts of thermal donors to examine if they affect the material properties after exposure to different high-temperature processes.

3.2 Experiment 1: material variation

Fig. 3a) shows the effective charge carrier lifetimes τ_{eff} measured by QSSPC at an injection level $\Delta n = 10^{15}$ cm^{-3} for the five materials and five different high-temperature process sequences after firing. The reference group "Ref" processed without any high-temperature steps is also stated. It is evident that the materials Mat3 and Mat4 with higher ρ_{Base} show higher τ_{eff} throughout the experiment due to less recombination active centres.

For easier interpretation, we calculate the lifetime factor β by dividing τ_{eff} per material and process sequence by the effective charge carrier lifetime $\tau_{eff,Ref}$ measured for the reference group per respective material:

$$\beta = \frac{\tau_{eff}}{\tau_{eff,Ref}}. \quad (1)$$

Fig. 3b) shows β for all groups.

Compared with $\tau_{eff,Ref}$, the measured τ_{eff} increases for all materials after a single $POCl_3$ diffusion by $1.6 \leq \beta \leq 2.4$ or after sequential BBr_3 + $POCl_3$ diffusions by $1.2 \leq \beta \leq 1.9$. Mat1 shows τ_{eff} up to $\tau_{eff} \approx 3$ ms after single $POCl_3$ diffusion and Mat3 and Mat4 even up to $\tau_{eff} \approx 6$ ms.

With BBr_3 diffusion being the second process (sequences: $POCl_3$ + BBr_3 and O_2 low + BBr_3), τ_{eff} is on the

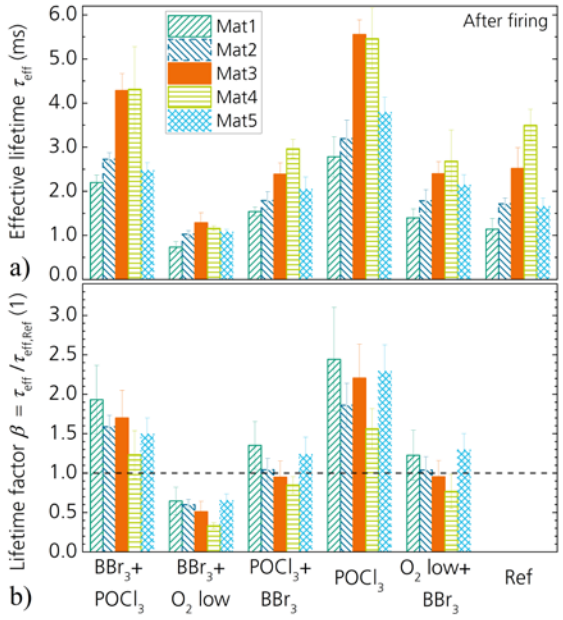

Fig. 3. a) Effective charge carrier lifetimes τ_{eff} measured by QSSPC at an injection level $\Delta n = 10^{15}$ cm^{-3} for five materials and five high-temperature process sequences as well as the reference group without any high-temperature process. The error bars represent the standard deviation of τ_{eff} measured on three to four samples at five positions each. The measurement positions are exemplarily marked in the first PL image in Fig. 4. b) Lifetime factor β as given in Eq. (1).

same level as the group Ref independent of whether there has been a $POCl_3$ diffusion or process O_2 low before BBr_3 diffusion. The factor β is found to be $\beta \approx 1$ for most of the materials or even $\beta \approx 1.3$ for Mat1 and Mat5.

Only the process sequence $BBr_3 + O_2$ low significantly reduces τ_{eff} by $0.3 \leq \beta \leq 0.7$ compared with group Ref. This degradation might be correlated with the O_2 low process as for all other combinations with BBr_3 diffusion the factor β is found to be $\beta \geq 1$ (see discussion above). A more detailed discussion will follow when discussing the PL images.

In the literature, it is reported that BBr_3 diffusion might lead to a significant degradation of τ_{eff} [9]. Here, we demonstrate that our optimized BBr_3 diffusion process is suitable for sequential diffusion processes. In combination with $POCl_3$ diffusion, τ_{eff} is at least the same as for group Ref, no matter which process order is used. When using sequential diffusion processes with $POCl_3$ first and then BBr_3, the phosphorus atoms can be driven-in even deeper during the BBr_3 diffusion. Our results indicate that both orders of the two diffusion processes are suitable for cell manufacturing, but for cell concepts that heavily rely on high bulk lifetimes, such as back contact back junction cells, $POCl_3$-last processing does appear to be advantageous.

Single $POCl_3$ diffusion as well as $POCl_3$-last processing lead to highest β values in this investigation. This might be correlated to a high gettering effect initiated by $POCl_3$ diffusion. In n-type silicon, impurities as Co, Cr, Ni and Fe might be recombination active and reduce τ_{eff} [10]. Phosphorus gettering is known to reduce these impurities in silicon wafers [11–14]. However, it is

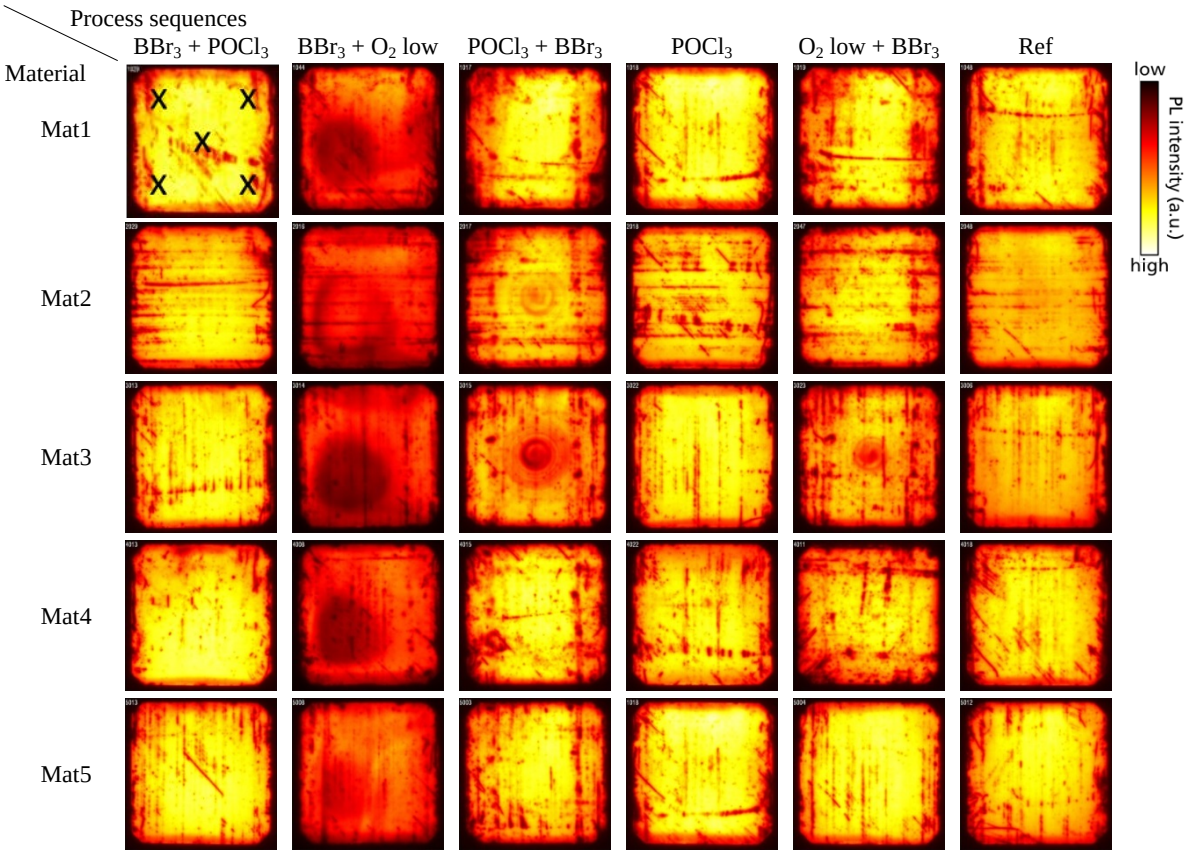

Fig. 4. Photoluminescence (PL) images for the five materials after the indicated high-temperature processes, etch back, passivation, and firing in the first experiment (one representative wafer per group). The PL intensity scale is the same for all images. The reference group Ref is also shown. At the top left PL image, the positions of the performed QSSPC measurements in Fig. 3 and Fig. 5 are exemplarily marked.

not clear which type of impurity is relevant for the n-type wafers used in our investigation.

However, all materials show the same trends for the different process combinations. Most of the materials and most of the process sequences show $\tau_{eff} > 1$ ms and $\beta \geq 1$. Mat4 shows the lowest β for all process sequences compared with the other materials. In comparison with Mat1, Mat2, and Mat5, the content of thermal donors is much higher (see Fig. 2). Thus, the thermal donors might affect τ_{eff} for Mat4. However, the high content of thermal donors for Mat3 does not seem to affect τ_{eff}.

In Fig. 4, PL images for the five materials after the high-temperature processes, as indicated in Fig. 3, are shown for one representative wafer per group after firing. Lines with lower PL intensity parallel to the wafer edges are caused by an insufficient saw-damage etching. Other scratches are attributed to wafer handling. The group Ref without any high-temperature processing is also shown in the very right column.

As already discussed, the process combination $BBr_3 + O_2$ low shows a degradation of τ_{eff} for all materials (Fig. 3). This can also be seen from the PL images. Wafers processed with $BBr_3 + O_2$ low show a dark area with lower PL intensity for all materials (Fig. 4). These dark structures might originate from an interaction of boron dopants and silicon interstitials injected by the O_2 low oxidation causing lower τ_{eff} compared with the reference group Ref. As these dark structures are visible in every material, they might be attributed to the process sequence and not to the material properties.

Mat2 and Mat3 show slight ring structures for the process sequence $POCl_3 + BBr_3$, and Mat3 also for the sequence O_2 low + BBr_3. Such ring structures are typically formed by oxygen precipitate formation [15]. These ring structures seem not to cause a significant degradation of τ_{eff} for Mat2. The QSSPC measurement performed in the wafer's center results in a similar τ_{eff} as the measurements performed at the other four positions. The wafers from Mat3 behave different. The QSSPC measurement in the wafer's center shows about 10% lower τ_{eff} compared to the measurement at the other four positions for both sequences with BBr_3-last processing.

In general, Mat3 with high content of thermal donors behaves similar as Mat1 with marginal content of thermal donors. Only for the process sequences with BBr_3-last processing small ring defects and a slight degradation of τ_{eff} occur in the wafer's centre for Mat3. But these ring defects are also visible for Mat2 which does hardly contain any thermal donors. Hence, thermal donors do not seem to significantly influence the materials' properties after exposure to specific high-temperature processes.

3.3 Experiment 2: high-temperature process sequence variation

For Mat1 and Mat2, the influence of the order of high-temperature processes with higher or lower temperature first as well as the applied gas atmosphere on τ_{eff} is investigated in more detail. The used process sequence is the same as in Fig. 1 and the measured τ_{eff} after firing are shown in Fig. 5a). Again, we calculate the lifetime factor β as given in Eq. (1); see Fig. 5b).

Again, it is obvious that the $POCl_3$ diffusion process being the second high temperature process shows an increased τ_{eff} compared with the reference group Ref. The factor β is calculated to be $\beta = 2.6$ and $\beta = 1.8$ for Mat1 and Mat2, respectively, when O_2 high is the preceding

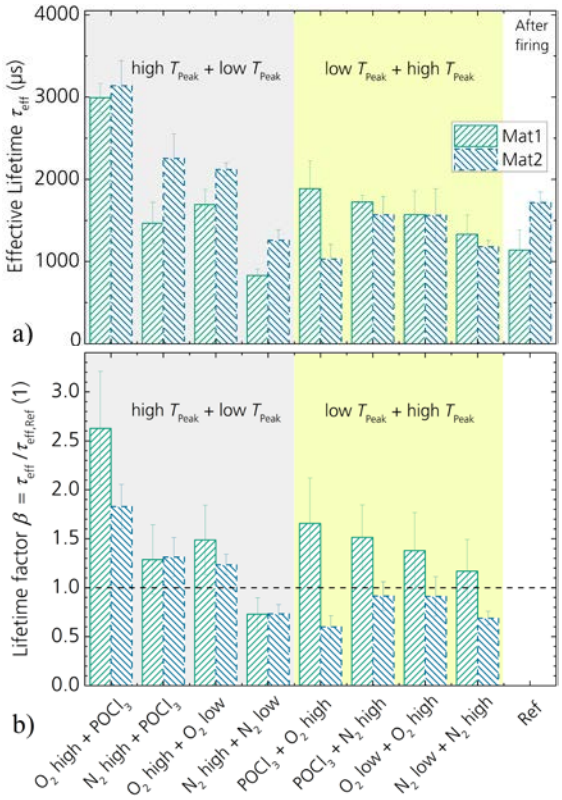

Fig. 5. a) Effective charge carrier lifetimes τ_{eff} measured by QSSPC at an injection level $\Delta n = 10^{15}$ cm^{-3} for two materials and the stated eight high-temperature process sequences, including the reference group without any high-temperature process. The error bars represent the standard deviation of τ_{eff} measured on three to four samples at five positions each. The measurement positions are exemplarily marked in the first PL image in Fig. 4. b) Lifetime factor β calculated as given in Eq. (1).

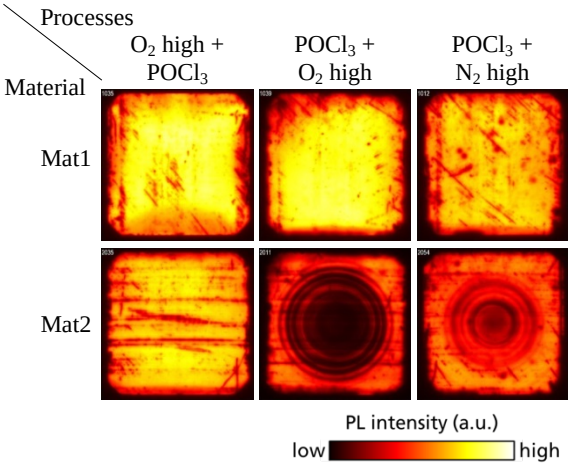

Fig. 6. Selected PL images for the two materials Mat1 and Mat2 taken after the indicated high-temperature processes, wet-chemical etch back, passivation and firing in the second experiment (one representative wafer per group). The PL intensity scale is the same as in Fig. 4.

high-temperature process. These β values are very similar as those calculated for Mat1 and Mat2 after a single $POCl_3$ diffusion (see section 3.2). But when N_2 high is the preceding high-temperature process before $POCl_3$

diffusion, β is reduced to $\beta = 1.3$ for both materials. Thus, the process O_2 high seems advantageous compared to N_2 high within the process sequence with following $POCl_3$ diffusion.

However, most of the process sequences with the high-temperature process at low temperature first and the process at high-temperature second yield $1.3 < \beta < 2.6$, only the sequence N_2 high + N_2 low shows a reduced τ_{eff} with $\beta \approx 0.7$ for both materials. The reason for this is not clear yet and further investigations are necessary.

Mat2 shows reduced τ_{eff} after process sequences with the higher temperature last (either O_2 or N_2 gas atmosphere). The factor β is found to be $0.6 < \beta < 0.9$ for Mat2 while $1.2 < \beta < 1.6$ for Mat1. The origin can be found in ring-like structures as apparent from the PL images in Fig. 6. For Mat2, O_2 high as well as N_2 high cause dark ring structures when being the second high-temperature process. The PL intensity in the ring area is even lower for O_2 high than for N_2 high. This is not only valid when $POCl_3$ is the first process but also for the groups with O_2 low + O_2 high or N_2 low + N_2 high (PL images not shown). As already mentioned, such ring structures are typically formed by oxygen precipitate formation [15]. But no ring structures are visible when O_2 high is the first process followed by either $POCl_3$ diffusion or O_2 low.

Furthermore, a lot of point-like structures appear especially for Mat1 after the process sequences featuring N_2 high as first process, as can be seen in the PL images in Fig. 7a) for representative wafers of material Mat1. The point-like structures are obvious for the sequences N_2 high + $POCl_3$ as well as N_2 high + N_2 low. These point-like structures might be attributed to oxide stacking faults [16]. But as $\beta = 2.6$ for Mat1 and the process sequence N_2 high + $POCl_3$, these point-like structures seem not to necessarily reduce τ_{eff}. When changing the process order to N_2 low + N_2 high, no point-like structures are visible.

Fig. 7b) shows the enlargement of the area marked in Fig. 7a). The PL images are taken as-cut, after process N_2 high, after $POCl_3$ diffusion and finally after passivation and firing. It is obvious that the point-like structures occur right after the N_2 high process. They stay at the same positions after $POCl_3$ diffusion as well as after passivation and firing. This indicates that the point-like structures can be related to the silicon bulk and not to the surface. The reason for these point-like structures as well as their impact on τ_{eff} need to be further investigated.

a) Process sequences

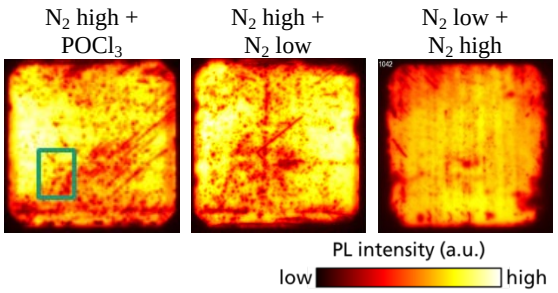

b) Enlargement of the area marked in a)

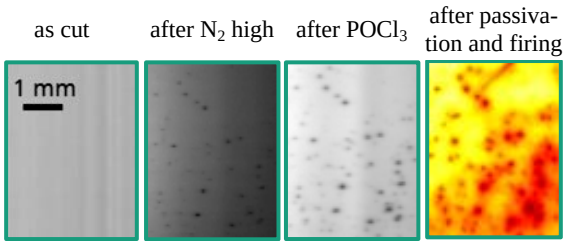

Fig. 7. a) Selected PL images for the material Mat1 taken after the indicated high-temperature process sequences, wet-chemical etch back, passivation, and firing in the second experiment (one representative wafer per group). The PL intensity scale is the same as in Fig. 4 and Fig. 6. b) Enlargement of the area marked in a). The PL images are taken as-cut, directly after the N_2 high tube furnace process, after $POCl_3$ diffusion and finally after passivation and firing. Different PL systems are used and the scaling is different.

4 SUMMARY AND CONCLUSION

The present work shows the impact of high-temperature processes at different temperatures, times, and gas atmospheres on n-type Czochralski-grown silicon wafers. Symmetric samples for lifetime measurements have been processed from wafers from five different ingots with different base resistivities and different contents of thermal donors. The high-temperature processes include BBr_3, $POCl_3$, O_2, or N_2 tube furnace processes, which are typically used for fabrication of high-efficiency n-type silicon solar cells.

The five materials react very differently to the high-temperature process sequences. Some process sequences have a positive impact on the effective charge carrier lifetimes τ_{eff} of these wafers, while other wafers show reduced τ_{eff}.

$POCl_3$-last processing has a positive impact on τ_{eff} for all materials. This might be related to a $POCl_3$ gettering that reduces recombination active impurities in the silicon wafers. After single $POCl_3$ diffusion, this results in $3\ ms \leq \tau_{eff} \leq 6\ ms$ for all investigated materials.

Our optimized BBr_3 diffusion process is suitable for sequential diffusion processes. In combination with $POCl_3$ diffusion, τ_{eff} is at least the same as for the reference group (no high-temperature processing), no matter which process order is used.

For process sequences with a moderate temperature in the first and a high temperature in the second process, some of the investigated wafers show ring structures, which likely originate from oxygen precipitate formation. These materials do not show any ring structures when changing the order of the high-temperature processes. Besides ring structures, also point-like structures are observed for some wafers which are subjected to process sequences with pure N_2 gas atmosphere at 1000°C as first process. These point-like structures might be attributed to oxide stacking faults, but they seem not to necessarily reduce τ_{eff}.

An appropriate order of the high temperature processes enables final charge carrier lifetimes that maintain or even exceed the values initially measured without any high-temperature processing.

ACKNOWLEDGEMENT

The authors would like to thank all colleagues at the Fraunhofer ISE Photovoltaic Technology Evaluation

Center (PV-TEC), especially U. Belledin, S. Maier and J. Stoffel.

REFERENCES

[1] K. Bothe, R. Sinton, J. Schmidt, "Fundamental boron-oxygen-related carrier lifetime limit in mono- and multicrystalline silicon", *Prog. Photovolt.: Res. Appl.*, vol. 13, pp. 287–296, 2005.

[2] A. Usami, Y. Fujii, K. Monoka, "The effect of swirl defects on the minority carrier lifetime in heat-treated silicon crystals", *J. Phys. D: Appl. Phys.*, vol. 10, no. 6, pp. 899–910, 1977.

[3] S. Werner, E. Lohmüller, S. Maier et al., "Process optimization for the front side of p-type silicon solar cells", *Proc. 29th EU PVSEC*, Amsterdam, Netherlands, 2014, pp. 1342–1347.

[4] A. Wolf, A. Kimmerle, S. Werner et al., "Status and perspective of emitter formation by $POCl_3$-diffusion", *Proc. 31st EU PVSEC*, Hamburg, Germany, 2015, pp. 414–419.

[5] S. Werner, E. Lohmüller, U. Belledin et al., "Optimization of BBr_3 diffusion processes for n-type silicon solar cells", *Proc. 31st EU PVSEC*, Hamburg, Germany, 2015, pp. 637–641.

[6] M. Spitz, U. Belledin, S. Rein, "Fast inductive inline measurement of the emitter sheet resistance in industrial solar cell fabrication", *Proc. 22nd EU PVSEC*, Milan, Italy, 2007, pp. 47–50.

[7] Seiffe J., Weiss L., Hofmann M. et al., "Alternative rear surface passivation for industrial cell production", *Proc. 23rd EU PVSEC*, Valencia, Spain, 2008.

[8] R. C. Newman, "Thermal donors in silicon: oxygen clusters or self-interstitial aggregates", *J. Phys. C: Solid State Phys. (Journal of Physics C: Solid State Physics)*, vol. 18, no. 30, pp. 967–972, 1985.

[9] M. A. Kessler, T. Ohrdes, B. Wolpensinger et al., "Charge carrier lifetime degradation in Cz silicon through the formation of a boron-rich layer during BBr_3 diffusion processes", *Semiconductor Science and Technology*, vol. 25, no. 5, pp. 1–9, 2010.

[10] J. Schmidt, B. Lim, D. Walter et al., "Impurity-related limitations of next-generation industrial silicon solar cells", *IEEE J. Photovoltaics*, vol. 3, no. 1, pp. 114–118 ,

[11] S. M. Myers, M. Seibt, W. Schröter, "Mechanisms of transition-metal gettering in silicon", *J. Appl. Phys.*, vol. 88, no. 7, pp. 3795–3819, 2000.

[12] M. Seibt, A. Sattler, C. Rudolf et al., "Gettering in silicon photovoltaics: current state and future perspectives", *phys. stat. sol. (a)*, vol. 203, no. 4, pp. 696–713, 2006.

[13] M. B. Shabani, T. Yamashita, E. Morita, "Metallic impurities in mono and multi-crystalline silicon and their gettering by phosphorus diffusion", *214th ECS Meeting*, Honolulu, HI, 2008, pp. 179–193.

[14] J. Schön, H. Habenicht, W. Warta et al., "Chromium distribution in multicrystalline silicon: comparison of simulations and experiments", *Prog. Photovolt: Res. Appl.*, pp. 676–680, 2012.

[15] A. Borghesi, B. Pivac, A. Sassella et al., "Oxygen precipitation in silicon", *J. Appl. Phys.*, vol. 77, no. 9, pp. 4169–4244, 1995.

[16] J. D. Murphy, M. Al-Amin, K. Bothe et al., "The effect of oxide precipitates on minority carrier lifetime in n-type silicon", *J. Appl. Phys.*, vol. 118, no. 21, p. 215706, 2015.